A Kinetic Model of Nitric Oxide Formation During Pulverized Coal Combustion

A mathematical model of nitric oxide (NO) formation during pulverized coal combustion was developed from a proposed kinetic mechanism involving 12 overall chemical reactions. Most significantly, the model describes the complex conversion of coal bound nitrogen compounds to NO during combustion. The predictions of the model compare favorably with literature data obtained in well defined laboratory combustors firing gaseous fuels doped with organic nitrogen additives, as well as with data obtained in laboratory coal combustors. The predictions of the model are in qualitative agreement with trends observed in practical coal combustors.

J. W. MITCHELL
and
J. M. TARBELL
Department of Chemical Engineering and
Center for Air Environment Studies
Pennsylvania State University
University Park, PA 16802

SCOPE

A major class of air pollutants evolved during coal combustion is the oxides of nitrogen—commonly referred to as NO_x. Nitric oxide (NO), the major species emitted in the burned gases of coal combustion processes, is derived from two sources—the molecular nitrogen in the combustion air and the organically bound nitrogen in the coal. The temperature sensitive mechanism of oxidation of molecular nitrogen to NO_x ("thermal NO_x" mechanism) is now well understood, and combustion modification strategies for NO_x control aimed at reducing peak flame temperatures have been successfully applied to gas and oil combustion processes. The temperature insensitive mechanism of fuel bound nitrogen conversion to NO_x ("fuel NO_x" mechanism) has been more difficult to unravel because it involves both homogeneous and heterogeneous reactions which occur on a time scale comparable to that of combustion reactions. The fuel NO_x picture is further complicated by the diversity of chemical forms in which the fuel bound nitrogen arises.

Since "fuel NO_x" is the major source of NO_x in practical coal combustion systems, there is considerable impetus to understand the mechanism and kinetics of its formation. A kinetic model is particularly important since combustion modification strategies, which are considered the most practical approach to NO_x control, generally exploit some distinctive kinetic feature of the conversion mechanism (e.g., temperature sensitivity in the case of molecular nitrogen conversion). The principal objective of the present work was to develop a quantitative mathematical model based on a chemical mechanism and associated kinetics which would adequately describe NO_x formation during pulverized coal combustion.

CONCLUSIONS AND SIGNIFICANCE

An overall kinetic mechanism involving 12 reactions has been developed to describe the formation of both fuel and thermal NO_x during the combustion of pulverized coal. Rate expressions and rate constants for each reaction (Table 1) have been determined. The coal combustion kinetics were extracted mainly from the literature while the fuel NO_x kinetics were derived through numerical simulation and regression of experimental data obtained in well defined, idealized reactor systems. The gas phase portion of the model has accurately predicted the NO_x formation from fuel nitrogen additives in both jet-stirred and Meker-type combustors as well as the low temperature reduction of NO by NH_3 as observed in the EXXON "thermal DeNO_x" process. The complete coal combustion—NO_x formation model (Table 1) was tested against experimental data from a bituminous coal laboratory burner with a coaxial injector nozzle. The simulations compared favorably with the experimental data—discrepancies being attributed to imperfect micromixing in the experimental diffusion flame which was not accounted for in the (kinetic) model.

In conclusion, the kinetic model of NO_x formation developed in this work is in quantitative agreement with well defined laboratory combustor data and in qualitative agreement with known trends in practical combustors. It may now be combined with flow and heat transfer models to provide an overall system model for simulation of pulverized coal combustors and prediction of their emission characteristics as a function of operating and design variables.

INTRODUCTION

The formation of the oxides of nitrogen (NO_x) from fuel bound nitrogen during the combustion of heavy oils and coal is a complex process involving both homogeneous and heterogeneous reactions and a wide variety of fuel nitrogen compounds. A considerable body of experimental work aimed at elucidating the homogeneous gas phase aspects of the conversion process has appeared in recent years (Fenimore, 1972; de Soete, 1975; Fenimore, 1976; Morley, 1976; Haynes, 1977; Muzio et al., 1977; Cortlett et al., 1979). The heterogeneous processes which accompany pulverized coal combustion have also been the subject of recent investigation (Pershing and Wendt, 1977; Pohl and Sarofim, 1977; Wendt and Pershing, 1977). A fairly coherent picture of the overall conversion mechanism emerges from this recent work, but a mathematical model which quantitatively accounts for all of the major kinetic events has not appeared in the literature. Such a model could be combined with flow and heat transfer models to allow simulation of the NO_x

0001-1541-82-5255-0302-$2.00.

TABLE 1. PROPOSED KINETIC MECHANISM

Stoichiometry	*Rate Form**	*Rate Constants*
(1a) $C(s) + \frac{1}{2}O_2 \rightarrow CO$	$\frac{dW_c}{dt} = \frac{-k_s k_d}{k_s + k_d} P_{O_2}\, Sext$	$k_d = 1.28 \times 10^{-3}\,(T_m/1{,}600)^{0.75}/d$
		$k_s = 8.71 \times 10^3 \exp(-35{,}700/RT)$ for $T < 1{,}500$ K
(1b) $N_c(S) + \frac{1}{2}O_2 \rightarrow NO$	$\frac{DN_{\underline{C}}}{dt} = \frac{N_{\underline{C}}}{W_{\underline{C}}}\frac{dW_{\underline{C}}}{dt}$	$k_s = 32.1 \exp(-19{,}000/RT)$ for $T > 1{,}500$ K
(2) $CO + \frac{1}{2}O_2 \rightleftharpoons CO_2$	$\frac{d[CO]}{dt} = -k_2[CO][O_2]^{1/2}[H_2O]^{1/2}$	$k_2 = 1.3 \times 10^{14} \exp(-30{,}000/RT)$
(3) $VM(s) \rightarrow C_mH_B$	$\frac{dV}{dt} = k_3(V_\infty - V)$	$k_3 = 2.08 \times 10^4 \exp(-22{,}000/RT)$
(4) $C_mH_B + \frac{m}{2}O_2 \rightarrow mCO + \frac{B}{2}H_2$	$\frac{d[C_mH_B]}{dt} = \frac{-2}{m}k_4'\frac{P^2}{T^{1.5}}f_{C_mH_B}f_{O_2}$	$k_4 = 3.39 \times 10^{10} \exp(-40{,}000/RT)$
(5) $N_c(s) \rightarrow HCN$	$\frac{dN_c}{dt} = -k_5 N_c \frac{VM^b}{V_\infty}$	$k_5 = 2.63 \times 10^5 \exp(-34{,}100/RT)$
		$b = 0.364$
(6) $NH_3 + O_2 \rightarrow NO + H_2O + \frac{1}{2}H_2$	$\frac{d[NH_3]}{dt} = \frac{-k_6 y_{NH_3} y_{O_2}}{1 + k_{den} y_{O_2}}\frac{P}{R'T}$	$k_6 = 3.48 \times 10^{20} \exp(-100{,}000/RT)$
		$k_{den} = 6.90 \times 10^{-6} \exp(42{,}000/RT)$
(7) $NH_3 + NO \rightarrow N_2 + H_2O + \frac{1}{2}H_2$	$\frac{d[NH_3]}{dt} = -k_7 y_{NH_3} y_{NO}\frac{P}{R'T}$	$k_7 = 6.22 \times 10^{14} \exp(-55{,}000/RT)$
(8) $N_2 + O_2 \rightleftharpoons 2\,NO$	$\frac{d[NO]}{dt} = \frac{2k_{17}K_o\left(\frac{P}{R'T}\right)^{1/2}[O_2]^{1/2}[N_2] - 2\frac{k_{-17}k_{-18}}{k_{18}}K_o\left(\frac{P}{R'T}\right)^{1/2}[NO]^2[O_2]^{-1/2}}{1 + \frac{k_{-17}[NO]}{k_{18}[O_2]}}$	$k_{17} = 7.8 \times 10^{13} \exp(-75{,}500/RT)]$
		$k_{-17} = 1.69 \times 10^{13}$
(9) $HCN + H_2O \rightarrow NH_3 + CO$	$\frac{d[HCN]}{dt} = -k_9 y_{HCN} y_{O_2}\frac{P}{R'T}$	$k_{18} = 1.4 \times 10^9\, T \exp(-6{,}260/RT)$
(10) $NO + \frac{1}{m}C_mH_B + \left(\frac{3 - B/m}{2}\right)H_2 \rightarrow HCN + H_2O$	$\frac{d[HCN]}{dt} = k_{10} y_{NO} y_{C_MH_B}\frac{P}{R'T}$	$k_{18} = 1.4 \times 10^9\, T \exp(-38{,}300/RT)$
		$K_o = 3.6 \times 10^3 \exp(-61{,}800/RT)$
(11) $C(s) + NO \rightarrow CO + \frac{1}{2}N_2$	$\frac{dW_{\underline{C}}}{dt} = -k_{11} y_{NO} S_{ext}\frac{P}{R'T}$	$k_9 = 1.94 \times 10^{15} \exp(-78{,}400/RT)$
(12) $H_2 + \frac{1}{2}O_2 \rightleftharpoons H_2$	Assumed Equilibrated	$k_{10} = 1.00 \times 10^4$
		$k_{11} = 1.57 \times 10^8 \exp(-34{,}000/RT)$
		$K_w = \exp(3.95 + 2.97 \times 10^{-4}T + 2.87 \times 10^4/T - 1.41\, lnT)$

* Rates for (1a) and (11) in units of g/sec, for (1b) (3) and (5) in sec^{-1}, all others in gmol/cm^3/sec

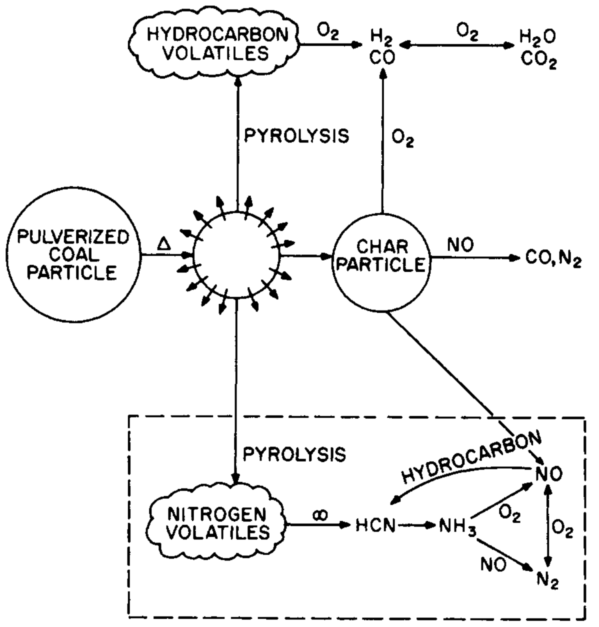

Figure 1. Kinetic model schematic.

emission characteristics of pulverized coal combustors.

In this work we have developed an overall, or, in the terminology of Weekman (1979), "lumped" kinetic model involving 12 reactions which accounts for many experimental facts. The data base for model discrimination and parameter estimation was provided by works available in the literature, many of which have already been mentioned. The methods involved numerical simulation of experimental systems which could be described as idealized reactors (mainly plug flow and stirred tank reactors) combined with nonlinear regression analysis.

KINETIC MODEL

The most important overall chemical reactions involved in NO_x formation during coal combustion are hypothesized to be those shown schematically in Figure 1. Coal pyrolysis, homogeneous hydrocarbon combustion, heterogeneous char combustion, fuel NO_x formation, and thermal NO_x formation are accounted for. The stoichiometry of the overall reaction mechanism employed in the kinetic model is summarized in Table 1 along with rate expressions and kinetic parameters which have either been extracted from the literature or determined in this work. Coal pyrolysis is described by reactions 3 and 5, and char combustion by rection 1a. The combustion of hydrocarbons evolved during coal devolatilization is accounted for by reactions 2, 4 and 12. Reaction 8 describes the thermal NO_x mechanism, while the fuel NO_x mechanism is represented by reactions 1b, 6, 7, and 9-11. The determination of the kinetics for each reaction is discussed below.

Coal Decomposition

When introduced into a hot (1,800 K) furnace, pulverized coal particles undergo thermal decomposition (pyrolysis). The compounds evolved during the period of rapid heating (10^4°C/second) are collectively referred to as volatile matter (VM). The amount of volatile matter released depends on coal type, heating rate, and ultimate temperature. The standard technique used to report volatile matter content of coal is the proximate analysis in which a coal sample is heated to 950° for seven minutes (ASTM, 1974). The amount of mass lost during this test is the proximate volatile matter content (VM_p).

Research, both experimental and theoretical, aimed at understanding pyrolysis phenomena has been extensive (Anthony and Howard, 1976). As a result, devolatilization data have been correlated by a wide variety of kinetic models, ranging from the single reaction, first order model of Badzioch and Hawksley (1970), to the multiple reaction model of Anthony et al. (1975) which employs a statistical distribution of activation energies. We have chosen a single reaction model to describe devolatilization in this work in order to minimize the total number of reactions essential for the description of coal combustion. However, the rate constants required by this method vary, for different coals, over orders of magnitude (Anthony and Howard, 1976). Therefore, the devolatilization rate constants for the particular coal being studied must be supplied to the model.

In this study, we assume that the volatile matter content of the residual char is zero, and thus, the devolatilization expression is given by

$$\frac{dV}{dt} = k_3(V_\infty - V) \qquad (1)$$

where

$$V_\infty = Q(VM_p) \qquad (2)$$

The volatile enhancement factor, Q, and thus the ultimate volatile yield, V_∞, depend on various factors (heating rate, temperature, coal type, size, etc.). For coals fired at high heating rates, the ultimate volatile yield typically exceeds the proximate volatile matter content by 10–50% (Anthony and Howard, 1976). Since the ASTM proximate volatile matter is usually known for a given coal, the additional model parameter needed to describe devolatilization is Q.

Although pyrolysis kinetics for any coal could be inserted into the model, most of the present analysis centers on a Pittsburgh seam hvA-bituminous coal. The literature on this coal is extensive, and contains sufficient data to evaluate the key characterizing parameters. Kobayashi et al. (1977) have carried out devolatilization studies on this coal, in which the kinetic rates were correlated with a first order expression, assuming a constant V_∞ of 70%. However, it is not apparent from their data that V_∞ is indeed independent of temperature. By allowing V_∞ to depend on temperature we have correlated the Kobayashi data with Eqs. 1 and 2. An ordinary differential equation solver based on Gear's method (Gear, 1971), and a nonlinear regression package based on Marquardt's method (Marquardt, 1963) were employed for this purpose. These two numerical methods were utilized for all of the simulation and correlation work described in this paper. The resulting correlation is compared to the data in Figure 2; the temperature dependence of V_∞ is shown in Figure 3; and the best fit kinetic parameters are listed in Table 1. The average relative error in the correlation is 13%.

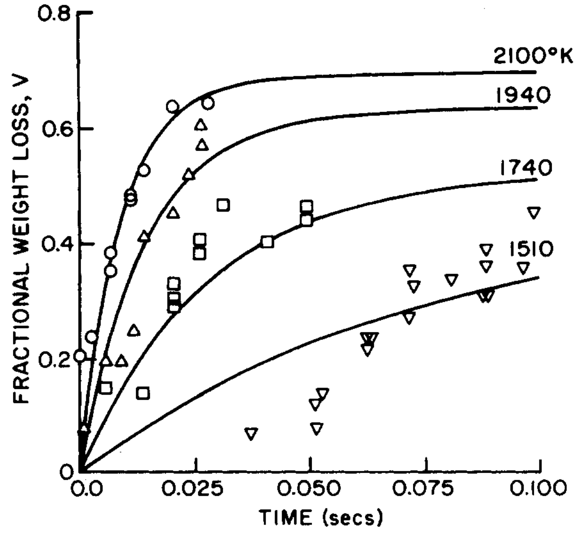

Figure 2. Volatile hydrocarbon evolution behavior. Data points from Kobayashi et al. (1977). Smooth curves from first order model.

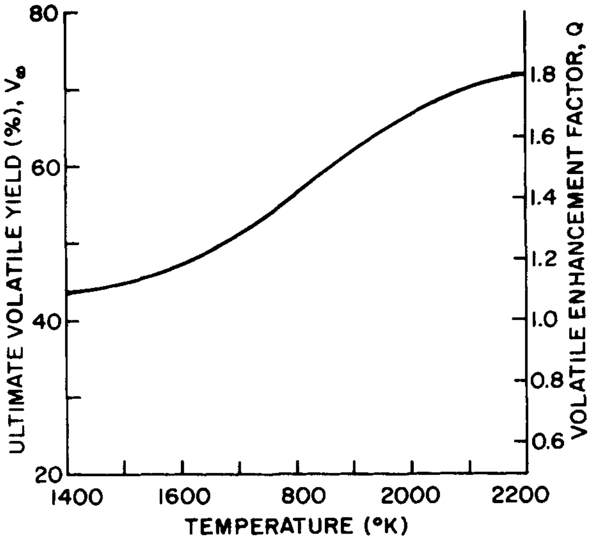

Figure 3. Effect of temperature on total yield of hydrocarbon volatiles.

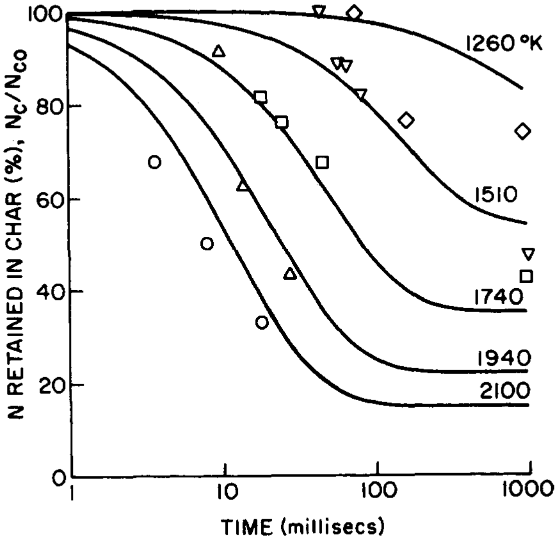

Figure 4. Volatile nitrogen evolution behavior. Data points from Pohl and Sarofim (1977). Smooth curves from model.

In addition to hydrocarbons, water and nitrogen evolution during pyrolysis are accounted for in the model. Coal bound moisture, held only by weak cohesive forces, is assumed to escape instantaneously upon particle injection into a hot furnace. Nitrogen evolution is, however, kinetically controlled (Pohl and Sarofim, 1977). Blair et al. (1977) studied the pyrolysis behavior of various coals at high heating rates and long residence times. They found that nitrogen evolution was more sensitive to temperature than hydrocarbon evolution, and that nitrogen species appeared to escape late in the devolatilization sequence. Workers at United Technologies Research Center (Solomon and Colket, 1978) conducted pyrolysis experiments on a variety of coals, and found trends similar to those discussed by Blair et al. (1977). In addition, they found that nitrogen evolution tends to parallel the overall volatile evolution, showing increased volatile nitrogen yield at higher temperatures. A study of nitrogen evolution by Pohl and Sarofim (1977) gives time resolved kinetic data, taken under conditions closely resembling those in coal flames. They heated small particles of the Pittsburgh seam coal to temperatures between 1,000 and 2,100 K at high heating rates and short residence times. Initial nitrogen evolution was correlated with a single first order reaction. While this approach adequately describes the early stages of nitrogen pyrolysis, it cannot predict the reduction in char retained nitrogen observed at increased temperatures. The apparent parallelism of nitrogen evolution with overall mass evolution has led us to the following rate expression for volatile nitrogen pyrolysis:

$$\frac{dNc}{dt} = -k_5 N_c \left(\frac{VM}{V_\infty}\right)^b \tag{3}$$

The constants in Eq. 3 were evaluated via batch reactor simulation using Eqs. 1–3 and numerical regression on the data of Pohl and Sarofim (1977). The best fit kinetic parameters are available in Table 1. As shown in Figure 4, Eq. 3 is able to describe both the increased rate and increased ultimate volatile nitrogen yield found at elevated temperatures. The average relative error in the regression was 10.3%.

The residual nitrogen remaining in the char ("char nitrogen") after devolatilization (which constitutes 20–30% of the total fuel nitrogen under typical pulverized coal combustion conditions) is released more slowly by a process which has been experimentally observed to parallel the char burnout (Pohl and Sarofim, 1977, Figure 4). However, the immediate fate of the char nitrogen (whether it is heterogeneously oxidized directly to NO or released as a -CN- or -HCN- fragment) has not been determined conclusively by experiments. We have adopted the view of Wendt and Schulze (1976) in which the residual nitrogen (assumed to be homogeneously distributed throughout the char) is oxidized directly to NO at a rate proportional to the char oxidation rate. Thus, the rate of char nitrogen oxidation (reaction 1a, Table 1) is expressed as follows:

$$\frac{dN_c}{dt} = \frac{N_c}{W_c}\frac{dW_c}{dt} \tag{4}$$

Char Combustion

The solid char (carbon) remaining after pyrolysis reacts heterogeneously with gas phase components such as O_2, CO_2, H_2O, and H_2. In hydrogen rich reducing atmospheres associated with gasification, all of these may be important, but in the present study focused on high temperature oxidizing conditions, only the char-O_2 reaction need be considered (Wen and Tone, 1978).

The mechanism of the char-O_2 reaction involves diffusive transport of oxygen through an external boundary layer to the particle surface, heterogeneous reaction at the surface, and subsequent diffusion of the products back through the boundary layer to the bulk gas phase. The rate determining step in the overall process depends on particle size and temperature. It is generally accepted (Essenhigh, 1977) that for particles larger than 100 micron in diameter, diffusion is rate controlling at normal combustion temperatures. Field (1969) has indicated that surface reaction control is evident for particles less than 50 microns in diameter. Of course, the diffusion limit is approached for all particles as the temperature is increased. In normal combustion systems, where diffusional and surface reaction rates are comparable, an overall rate expression combining the two effects is often employed (Lowe et al., 1977). Assuming the surface reaction to be first order, the char consumption rate is written as

$$\frac{dW_c}{dt} = \frac{-k_s k_d}{k_s + k_d} P_{O_2} S_{\text{ext}} \tag{5}$$

where P_{O_2} is the oxygen partial pressure in the bulk gas, S_{ext} is the total external surface area per unit mass of the char particles, and k_s and k_d are the surface reaction and diffusional coefficients, respectively. Field et al. (1967) have shown that

$$k_d = \frac{24\,\psi\,D_{O_2}}{d\,R'\,T_m} \tag{6}$$

where T_m is the mean temperature in the boundary layer and ψ is the mechanism factor which has a value of 1 if CO_2 is formed at the surface, and 2 if CO is formed at the surface. Field (1969) concluded that in most cases the principle surface product is CO, and expresses the diffusional coefficient as

$$k_d = 1.28 \times 10^{-3}\,(T_m/1{,}600)^{0.75}/d \tag{7}$$

In most experimental work, intraparticle diffusion effects have been lumped into the surface reaction coefficient. Field et al. (1967) summarized the work of various authors and suggested the following expression

$$k_s = 8.71 \times 10^3 \exp(-35700/RT) \tag{8}$$

for temperatures below 1,650 K. At higher temperatures, the data shows significant curvature when plotted in Arrhenius form, presumably due to intraparticle diffusion effects. Based on regression of the Field et al. (1967) data, the following Arrhenius expression is suggested for k_s at high temperatures (1,500-2,500 K):

$$k_s = 32.1 \exp(-19{,}000/RT) \tag{9}$$

While Eq. 5 describes the rate of burning, it alone is not adequate to fully describe the physical changes which occur during burnout. As a char particle burns, it undergoes variations in both diameter and density (Anson et al., 1971; Field, 1970). The parameters α and β defined below are used to describe this diameter and density variation

$$d/d_o = (W_c/W_{c_o})^{\alpha} \tag{10}$$

$$\rho/\rho_o = (W_c/W_{c_o})^{\beta} \tag{11}$$

It has been shown by Lowe et al. (1977) that for spherical particles

$$3\alpha + \beta = 1\,. \tag{12}$$

α and β, which may be determined experimentally, effectively describe the amount of internal burning of a char particle. When β is zero, there is only surface burning, and the description reduces to that of the so called "shrinking sphere" model. For constant diameter burning, β has a value of unity. In general, more porous chars have higher β values.

Many coal particles also change physically by swelling during the initial period of rapid heating. Experimental evidence suggests that swelling is usually mild (<10%) and occurs at a rate proportional to the extent of devolatilization (Baum and Street, 1971). By defining a swelling parameter, C_{sw}, as the maximum fractional amount of swelling, diameter and density variations for spherical particles are given by

$$d = d_0\left[1 + \left(1 - \frac{VM}{V\infty}\right)C_{sw}\right] \tag{13}$$

$$\rho = \rho_0 \Big/ \left\{\left[1 + \left(1 - \frac{VM}{V\infty}\right)C_{sw}\right]^3\right\} \tag{14}$$

The parameters β and C_{sw} have been shown to have a negligible effect on NO_x emissions (Mitchell, 1980).

Hydrocarbon Combustion

Data on the composition of gas phase products of coal pyrolysis is scarce, but limited data shows that the molecular weight of the products decreases with increasing temperature (Wen et al., 1973). Volatile products are usually divided into tars, gas, and water, and Menster et al. (1973) have shown that the tar fraction decreases to below 15% at typical combustion temperatures. It can be inferred from these studies that the majority of volatiles produced are low molecular weight hydrocarbons. Zimont and Trushin (1969) have discussed overall kinetics for hydrocarbon combustion and have concluded that the kinetic parameters describing propane/air and iso-octane/air mixtures are very similar. Based on these works, we have assumed that pyrolysis products exist as a single "average" hydrocarbon species (C_MH_B) whose combustion is described by the following overall rate (Zimont and Trushin, 1969):

$$\frac{d[C_MH_B]}{dt} = -\frac{2}{M}k_4\frac{P^2}{T^{1.5}}(f_{hc}f_{O_2}) \tag{15}$$

The mass rate of hydrocarbon combustion predicted by Eq. 15 is essentially independent of the hydrocarbon molecular weight. There is less than a 2% difference between the mass rate of methane and octane combustion. We have fixed $M = 8$ for our model with the parameter B determined by the ultimate and proximate analysis of the coal (Mitchell, 1980). The rate constant is available in Table 1.

It is generally accepted that the rate limiting step in hydrocarbon combustion is the oxidation of carbon monoxide. Howard et al. (1973) reviewed CO oxidation studies by various investigators. They obtained a global rate expression which adequately agrees with data representing various fuels, equivalence ratios, pressures, and temperatures in the range 840 to 2,360 K. The resulting global equation is

$$\frac{d[CO]}{dt} = -k_2[CO][O_2]^{1/2}[H_2O]^{1/2} \tag{16}$$

which can be used except at near equilibrium conditions where the reverse rate can be calculated from equilibrium analysis and thermochemical data (Mitchell, 1980).

The remaining homogeneous combustion reaction that we have included is the oxidation of H_2 to H_2O. Surprisingly, only one global kinetic study of this reaction is available in the literature (Sawyer and Glassman, 1969), and it concentrates on systems containing large amounts of excess air. The rate expression is zero order in O_2 concentration, and thus, it cannot be used in models of rich flames. Preliminary calculations confirmed our expectation that this reaction is very fast; therefore it has been assumed to be always in thermodynamic equilibrium. The equilibrium constant, K_w, is available in Table 1.

Thermal NO_x Formation

Thermal NO_x formation is now well understood, and the mechanism originally proposed by Zeldovich (1946)

$$O + N_2 \underset{k_{-17}}{\overset{k_{17}}{\rightleftharpoons}} NO + N \tag{17}$$

$$N + O_2 \underset{k_{-18}}{\overset{k_{18}}{\rightleftharpoons}} NO + O \tag{18}$$

accurately accounts for thermal NO_x formation in both fuel lean and fuel rich flames (Newhall and Shahed, 1973). Lavoie et al. (1970) have proposed that, in addition to the simple Zeldovich mechanism, the reaction

$$N + OH \rightarrow NO + H \tag{19}$$

may be significant, especially in fuel rich flames. Shock tube studies by Bowman (1971) have shown the dominance of reactions 17 and 18; thus reaction 19 is not considered in the present treatment.

Based on the Zeldovich mechanism the thermal NO_x formation rate, after invoking the "steady state approximation" for the nitrogen atom concentration, is given by (Westenberg, 1971)

$$\frac{d[NO]}{dt} = 2[O]\left\{\frac{k_{17}[N_2] - k_{-17}\,k_{-18}\dfrac{[NO]^2}{k_{18}[O_2]}}{\dfrac{1 + k_{-17}[NO]}{k_{18}[O_2]}}\right\} \tag{20}$$

which shows the sensitivity to O atom concentration. If the reaction

$$O_2 \rightleftharpoons O + O \tag{21}$$

is assumed to be in equilibrium, Eq. 20 reduces to

$$\frac{d[NO]}{dt} = \frac{2k_{17}K_o\left(\dfrac{P}{R'T}\right)^{1/2}[O_2]^{1/2}[N_2] - 2(k_{-17}k_{-18}/k_{18})K_o(P/R'T)^{1/2}[O_2]^{-1/2}[NO]^2}{1 + \dfrac{k_{-17}[NO]}{k_{18}[O_2]}} \tag{22}$$

where K_o is the equilibrium constant for oxygen dissociation. In assessing the validity of this assumption, it is important to note that the thermal mechanism is slow compared to hydrocarbon combustion, and most of the thermal NO_x formation occurs in the "post flame" region. It is well known that super-equilibrium free radical concentrations exist in the flame zone, but, as pointed out by Westenberg (1971), these excess concentrations disappear at a rate faster than NO is formed, thus deviations from rate (Eq. 22) are small. Finally, we should note that thermal NO_x formation is significant only at temperatures exceeding those found in typical pulverized coal systems (1,800 K) (Sarofim and Flagan, 1976). The rate constants (Jensen and Jones, 1978) and the equilibrium constant (JANAF) required by Eq. 22 are available in Table 1.

Fuel NO_x Formation

The fixation of atmospheric nitrogen by the thermal NO_x mechanism is highly sensitive to temperature, and studies have shown that in relatively cool coal flames less than 20% of the NO_x is formed via the thermal mechanism (Pershing and Wendt, 1977). In contrast, NO_x formation due to the oxidation of fuel bound nitrogen compounds has been found to be rather insensitive to flame temperature. And, while the thermal mechanism is well described by the relatively simple Zeldovich mechanism, recent research indicates that the fuel NO_x mechanism is much more complex (Vogt and Laurendeau, 1976). In view of the wide variety of coal types, and organically bound nitrogen compounds associated with them (Axworthy, 1975), it would appear a formidable task to realistically model fuel NO_x conversion. Fortunately, numerous experimental studies have revealed that fuel NO_x conversion is remarkably insensitive to the nature of the organic nitrogen compound (Fenimore, 1972; Sarofim et al., 1976). And, while perhaps incomplete, the "four centers" description of Haynes (1977) provides insight into the gas phase mechanism. In the Haynes view, the gas phase conversion is described by the interaction of four nitrogen centers: (1) the NH_i subsystem (N, NH, NH_2, NH_3), (2) the CN subsystem (mostly HCN), (3) NO, and (4) N_2. For the purpose of our global model, the four centers are represented by the molecular species NH_3, HCN, NO, and N_2.

The hypothesized interactions among the centers are shown schematically in Figure 1 and are listed in Table 1 as reactions 6–10. To determine the necessary kinetic parameters, the effects associated with each center were isolated by starting with N_2 and the thermal mechanism, and adding on the remaining centers in building block fashion. Fortunately, available experimental data in the literature allowed us to carry out this procedure. The interaction between the N_2 and NO centers is accounted for by the thermal mechanism which has been discussed above.

Reactions involved when the NH_i center is included are the oxidation of NH_i to NO and reduction to N_2 via NO. Fenimore (1976) has suggested that the NO destruction is due mainly to the reaction

$$NO + NH_2 \rightarrow N_2 + H_2O \qquad (23)$$

and, while not readily interpreted in terms of elementary reactions, the NO formation reaction is of the type

$$NH_i + Ox \rightarrow NO + \ldots\ldots \qquad (24)$$

where Ox is an appropriate gas phase oxidant. Haynes (1977a) has suggested that the NH_i subsystem (N, NH, NH_2, NH_3) is internally equilibrated. Thus, the use of a single NH_i species (NH_3) in a global scheme is justified.

In an attempt to describe fuel NO_x formation by oxidation and reduction reactions like reactions 6 and 7 of Table 1, de Soete (1975) correlated the oxidation rate with an expression that was of variable order dependence on oxygen concentration. He found that at low O_2 levels the rate appeared first order in oxygen, and that a zero order dependency best described the rate at high O_2 levels. He assumed the NO reduction rate to be first order in both fuel nitrogen species and NO.

To obtain kinetic parameters for the NH_i oxidation and reduction reactions, a set of data on a system that isolates the NH_i, NO, and N_2 interactions is required. The numerous reported experimental results for fuel nitrogen doped hydrocarbon flames are of limited use, due to the presence of HCN and hydrocarbon fragments in the flame zone. A useful experimental system for study of the NH_i reactions is the thermal *De*NO_x (PAT report, 1977) system in which ammonia is injected into the burnt gases of lean hydrocarbon flames. Due to the presence of excess oxygen, the gases at the injection site are nearly devoid of HCN and hydrocarbon species. An extensive data set, covering a broad range of temperatures and ammonia-NO stoichiometries, is available in the work of Muzio et al. (1977). They burned CH_4 with excess air in a plug flow combustor, injected NH_3 into the burned gases, and measurd the NO concentration upstream and downstream of the injection point.

Originally, we expected that de Soete's global kinetics could be incorporated directly into simulation of these relatively low temperature experiments. But, de Soete's kinetics failed to predict the strong temperature dependence of the selectivity of the parallel NH_3 reactions observed by Muzio et al. Therefore, we postulated new global kinetic forms (Eqs. 25 and 26) to describe both the oxidation and reduction of the NH_i system.

$$\frac{d[NH_3]}{dt} = \frac{-k_6 y_{NH_3} y_{O_2}}{1 + k_{den}\, y_{O_2}} \frac{P}{R'T} \qquad (25)$$

$$\frac{d[NH_3]}{dt} = -k_7\, y_{NH_3}\, y_{NO} \frac{P}{R'T} \qquad (26)$$

Equation 25 allows for the oxygen dependence observed by de Soete while providing additional flexibility in temperature dependence through the Arrhenius parameter k_{den}.

The experiments of Muzio et al. (1977) were simulated (Gear's method) by a plug flow reactor model incorporating the thermal NO_x kinetics of Eq. 22 along with Eqs. 25 and 26. Nonlinear regression (Marquardt algorithm) of the entire data set resulted in the best fit constants recorded in Table 1. Figure 5 compares the predictions of the best fit plug flow model with the experimental data. The average relative deviation of the best fit simulation data from the experimental data is 13.7%. The rather pronounced temperature well is quite adequately described by the model.

The final nitrogen center to be considered is the CN subsystem (HCH, CN etc.) which, like the NH_i subsystem, is assumed to be internally equilibrated. This subsystem is represented by the single species HCN in our model. Reactions leading to the formation, and destruction of this center are discussed below.

Nitrogen bearing heterocyclic compounds are evolved from coal

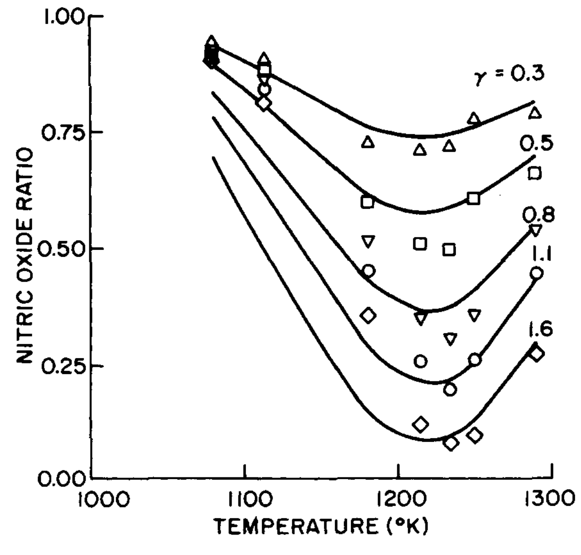

Figure 5. NO_x reduction during ammonia injection. Data points from Muzio et al. (1977). Smooth curves from plug flow model. Nitric oxide ratio is ratio of NO_x after ammonia injection to initial NO concentration. γ is the injection stoichiometry ($[NH_3]/[NO]$).

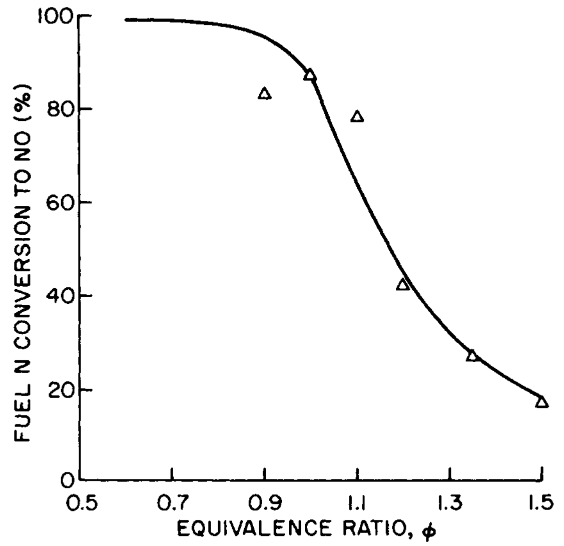

Figure 6. NO_x formation in a jet-stirred combustor. Data from Corlett et al. (1979). Smooth curve from CSTR model. Nominal combuster residence time of 13 ms.

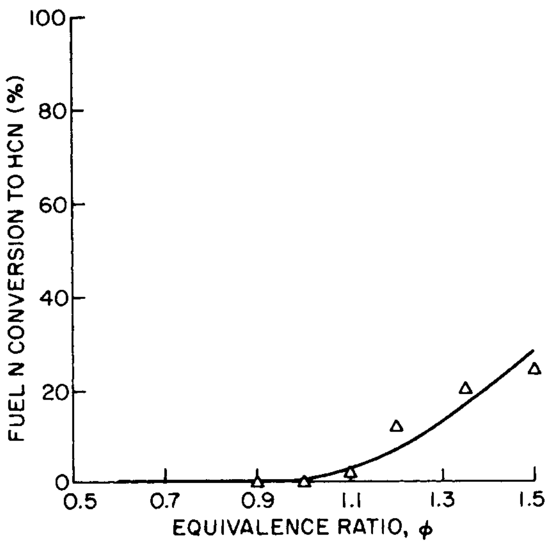

Figure 7. HCN formation in a jet-stirred combustor. Data from Corlett et al. (1979). Smooth curve from CSTR model. Nominal combustor residence time of 13 ms.

by pyrolysis and char decomposition during coal combustion. It has been suggested that at high temperatures, ring rupture at the heterocyclic site is possible, and reactions such as

$$C_5H_5N \xrightarrow[\Delta]{} HCN + C_4H_4 \tag{27}$$

may yield hydrogen cyanide directly (Sternling and Wendt, 1972). Studies in hydrocarbon flames doped with nitrogen compounds (Haynes, 1977) indicated that HCN is the dominant nitrogenous species formed in the reaction zone, with nearly 100 percent conversion of fuel N to HCN (Morley, 1976). Since reactions like eq. 27 are exceedingly fast, we have assumed an infinite rate for the conversion of nitrogen volatiles to HCN. The subsequent (rate limiting) decay of HCN yields the NH_i species necessary to propagate the fuel NO_x mechanism.

HCN may also form as a result of hydrocarbon interactions with the NO center. Reactions of the type

$$CH_3 + NO \rightarrow HCN + H_2O \tag{28}$$

have been proposed (Haynes, 1977) to account for NO reduction by hydrocarbons, which is significant only in rich flames (Corlett et al. 1979). This process is described in the overall model by reaction 10 of Table 1, whose rate is expressed as

$$\frac{d[\mathrm{HCN}]}{dt} = k_{10} y_{\mathrm{NO}} y_{\mathrm{C}_m\mathrm{H}_B} \frac{P}{R'T} \tag{29}$$

Flame studies have shown that as HCN decays, NH_i concentrations increase (Haynes, 1977) due to reactions such as (Morley, 1976)

$$CN + OH \rightarrow NH + CO \tag{30}$$

or

$$O + HCN \rightarrow NCO + H \rightarrow NH + CO \tag{31}$$

In any case, the decay of the HCN subsystem is initiated by the attack of an oxidizing agent. This conversion of the HCN center to the NH_i center is described in overall fashion by Eq. 9 of Table 1, with a rate of the form

$$\frac{d[\mathrm{HCN}]}{dt} = -k_9 y_{\mathrm{HCN}} y_{\mathrm{O_2}} \frac{P}{R'T} \tag{32}$$

While qualitative data on fuel NO_x formation is abundant in the literature, quantitative data from well defined reaction systems, suitable for determination of the kinetic parameters in Eqs. 29 and 32, is scarce. However, the study of Corlett et al. (1979) in a Longwell reactor (jet stirred reactor) provides the essential data. In these experiments, Cortlett et al. premixed pyridine with propane, argon, and oxygen and combusted the mixture at temperatures ranging from 1500 to 1900°K, at equivalence ratios from 0.9 to 1.5. Reactor residence times and a complete nitrogen balance (N_2, NO, HCN, NH_3) were given.

The Longwell reactor was modeled as a continuous stirred tank reactor (CSTR) incorporating kinetics for propane partial oxidation (Zimont and Trushin, 1969) and reactions 2, 6–10 and 12 of Table 1. For each experimental run, a "best" pair of rate constants (k_9 and k_{10}) was determined by simulation with the CSTR model. The CSTR model was solved by integrating the transient equations to steady state (Gear's method). Results of this procedure were correlated with Arrhenius expressions, and linear regression of the data led to the k_9 and k_{10} values reported in Table 1.

The CSTR model (with the kinetics of Table 1) was able to predict both the decreased conversion of fuel nitrogen (in pyridine) to NO and the increased conversion to HCN observed at increasingly rich conditions. Figures 6 and 7 provide a comparison of model predictions and experimental data for a nominal residence time of 13 millisecond. The model also agreed favorably with data at longer residence times and at higher fuel nitrogen concentrations (Mitchell, 1980).

As a final check on the gas phase mechanism and kinetics, data from premixed CH_4/air flames doped with fuel nitrogen compounds in a Meker-type burner (Sarofim et al., 1976) was simulated. The data was reported as percent fuel nitrogen (various additives) converted to NO at various equivalence ratios and additive concentrations. The Meker burner was modeled as a plug flow reactor (PFR) incorporating the same kinetics as the prior CSTR model, except that the CH_4 partial oxidation kinetics of Williams et al. (1969) were employed. Figure 8 compares the PFR model predictions with the experimental data at an additive concentration of 0.5 wt.%. Agreement is very favorable, with the model predicting the drastic reduction of NO formation under fuel rich conditions. This completes our discussion of the homogeneous reactions involved in the NO mechanism.

Beer et al. (1977) have proposed that in coal combustion systems a heterogeneous reaction between NO and char particles will reduce the NO formed. While very significant under fluidized bed conditions, this reaction may also be important in pulverized coal flames. Products of the uncatalyzed process include CO, CO_2, and N_2 formed through reactions such as

$$C + 2NO \rightarrow CO_2 + N_2 \tag{33}$$

$$C + NO \rightarrow CO + \tfrac{1}{2} N_2 \tag{34}$$

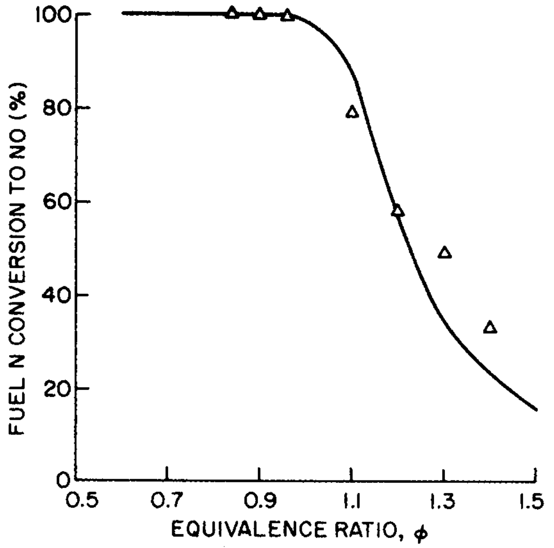

Figure 8. NO_x formation in a meker-type burner. Data from Sarofim et al. (1976). Smooth curve from PFR model.

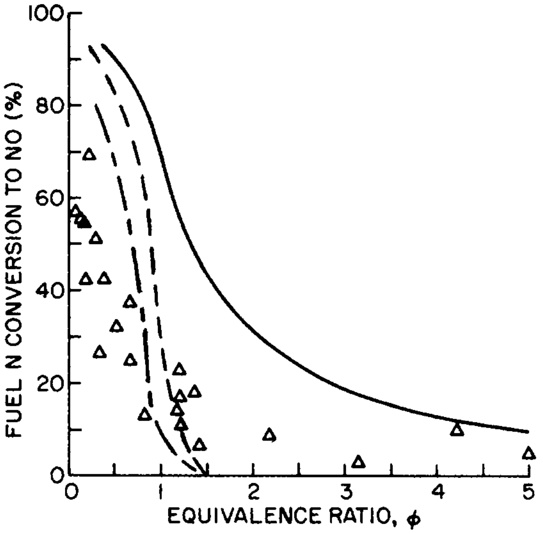

Figure 9. NO_x production in an isothermal coal combustor. Data (1,500 K) from Pohl and Sarofim (1977). Smooth curves from PFR model. —— $k_{11} = 0$; - - - $k_{11} = 1.57 \times 10^8 \exp(-34{,}000/RT)$; — - — $k_{11} = 6.28 \times 10^8 \exp(-34{,}000/RT)$.

The reaction is modeled as first order in NO concentration and proportional to the char surface area available. The rate constant given by Horio et. al. (1977) is recorded in Table 1 (reaction 11). Preliminary tests at 1800°K and short residence times characteristic of pulverized coal flames indicate that the char/NO reaction is quite significant. This point is considered in detail in the next section.

OVERALL MODEL VERIFICATION AND MIXING EFFECTS

Rationale for the mechanisms and kinetics in Table 1 has been presented. It remains to test the kinetic model on a well defined system involving both NO formation and coal combustion. Pohl and Sarofim (1977) measured NO formation during combustion of a Pittsburgh seam coal (whose pyrolysis characteristics we described in an earlier section) in an electrically heated resistance furnace. Nearly mono-sized particles were burned in diffusion flames created by feeding the coal and 15% of stoichiometric oxygen requirement through a nozzle on the axis of the furnace. The remaining oxygen was fed coaxially without swirl. Helium replaced nitrogen as a diluent. We simulated these experiments with a PFR model incorporating the complete set of kinetics in Table 1 as well as several variations of the char/NO kinetics. The coal characterizing parameters were taken from Kobayashi et al. (1977). The volatile enhancement factor, Q, was set at 1.1 (cf. Figure 3), and mild swelling and internal burning effects were simulated by setting $C_{sw} = 0.05$ and $\beta = 0.05$.

Figure 9 displays the experimental data and several model predictions for 50 μm particles burning at 1,500 K. The solid line is the prediction when the char/NO reaction is not operative ($k_{11} = 0$). The broken lines employ the k_{11} of Horio et al. (1977) listed in Table I as well as a value four times that of Horio et al. (1977) which was used recently by Rajan and Wen (1980) in a fluidized bed model. It is clear that the char/NO reaction significantly reduces NO levels, particularly under fuel rich operating conditions, and that predictions of NO emissions are quite sensitive to the rate of the char/NO reaction.

The remaining discrepancy between the experimental data and the model predictions including the char/NO reaction we attribute in large measure to imperfect micromixing—an effect not accounted for in our PFR model. A qualitative explanation of the micromixing effect is possible if we imagine a local distribution of fuel/air equivalence ratio regions in the combustor—some fuel rich and some fuel lean relative to the mean equivalence ratio (Tarbell and Petty, 1977). In regions where the curvature of y_{NO} versus ϕ (i.e., $\partial^2 y_{NO}/\partial\phi^2$) under perfect mixing conditions is positive, imperfect mixing will reduce NO, while the trend is reversed when the curvature is negative. This argument applied to the results in Figure 9 indicates that imperfect mixing will reduce NO emissions under overall fuel lean operating conditions with the trend reversed under fuel rich conditions.

In fact, it is quite well known that poor mixing leads to reduced NO formation under fuel lean operating conditions in both practical and laboratory combustors (Wendt and Pershing, 1977). In addition, tangentially fired coal boilers (low mixing intensity) produce significantly less NO than opposed wall fired coal boilers (high mixing intensity) under normal operating conditions as shown clearly in Tables 2 and 4 of Sarofim and Flagan (1976). The same Table 2 shows a consistent reduction in NO emissions with reduction in boiler load which is accompanied by poorer mixing.

In conclusion, we feel that our model adequately accounts for the important chemical kinetic events in the conversion of fuel bound nitrogen during pulverized coal combustion. However, a complete system model will have to in addition account for: (1) the important effect of microscale segregation and associated micromixing; (2) imperfect macromixing as described by the residence time distribution of each feed stream; and (3) non-isothermal effects as described by energy balances for both the gas and particle phases.

ACKNOWLEDGMENT

Support of this work by the Mick A. Naulin Foundation, Ltd. is gratefully acknowledged. We would like to thank Ken Li of the Chemical Engineering Department at Penn State for his work on the char/NO reaction.

NOTATION

b = correlational constant in Eq. 3
C_{sw} = fractional swelling constant
$CSTR$ = continuous stirred tank reactor
d = diameter of coal (char) particle (cm)
d_o = initial diameter of coal particle (cm)
D_{O_2} = diffusivity of oxygen in combustion gases (cm^2/s)
f_{X_2} = gas phase mass fraction of compound X_2
K_o = oxygen dissociation equilibrium constant
N_c = nitrogen contained in coal (g/g coal)
N_{co} = initial nitrogen content of coal (g/g coal)
P = pressure (atm)

PFR = plug flow reactor
P_{O_2} = partial pressure of oxygen (atm)
Q = volatile enhancement factor
$R(R')$ = universal gas constant, 1.987 cal/gmol-K(82.057 cm^3 atm/gmol-K)
S_{ext} = coal surface area (cm^2)
t = time (s)
T = temperature (K)
T_m = temperature in coal boundary layer (K)
V = volatile matter evolved into gas phase (g/g coal)
VM = volatile matter contained in coal (g/g coal)
VM_p = proximate volatile matter content of coal (g/g coal)
V_∞ = ultimate volatile matter yield of coal (g/g coal)
W_c = char weight (g)
W_{co} = initial weight of coal (g)
y_{x_2} = gas phase mole fraction of compound X_2
$[X_2]$ = gas phase concentration of compound X_2 (gmol/cm^3)
α = size variation parameter for char burnout
β = density variation parameter for char burnout
γ = NH_3/NO ratio in NH_3 injection
ρ = particle density (g/cm^3)
ρ_o = initial particle density (g/cm^3)
ϕ = equivalence ratio
ψ = mechanism factor for char/O_2 reaction
τ = mean residence time

LITERATURE CITED

Anson, D., F. D. Moles, and P. J. Street, "Structure and Surface Area of Pulverized Coal During Combustion," *Comb. Flame*, **16**, 265 (1971).

Anthony, D. B., and J. B. Howard, "Coal Devolatilization and Hydrogasification," *AIChE J.*, **22** (4), 625 (1976).

Anthony, D. B., J. B. Howard, H. C. Hottel, and H. P. Meissner, "Rapid Devolatilization of Pulverized Coal," Fifteenth Symposium (International) on Combustion, p. 1303, The Combustion Institute (1975).

ASTM, "Standards on Coal and Coke," Annual Book of ASTM Standards, American Society for Testing and Materials, Philadelphia, PA (1974).

Axworthy, A. E., "Chemistry and Kinetics of Fuel Nitrogen Conversion to Nitric Oxide," *AIChE Symp. Ser.*, No. 148, **71**, 43 (1976).

Badzioch, S. and P. G. W. Hawksley, "Kinetics of Thermal Decomposition of Pulverized Coal Particles," *Ind. Eng. Chem. Process Des. Develop.*, **9**(4), 521 (1970).

Baum, M. M. and D. J. Street, "Predicting the Combustion Behavior of Coal Particles," *Comb. Sci. Tech.*, **3**, 231 (1971).

Beér, J. M., A. F. Sarofim, L. K. Chan, and A. M. Sprouse, "NO Reduction by Char in Fluidized Combustion," Proc. Fifth Int. Conference on Fluidized Bed Combustion, **II**, Washington, DC (1977).

Blair, D. W., J. O. L. Wendt, and W. Bartok, "Evolution of Nitrogen and Other Species During Controlled Pyrolysis of Coal," Sixteenth Symposium (International) on Combustion, p. 475, The Combustion Institute (1977).

Bowman, C. T., "Investigation of Nitric Oxide Formation Kinetics in Combustion Processes: The Hydrogen-Oxygen-Nitrogen Reaction," *Comb. Sci. and Tech.*, **3**, 37 (1971).

Corlett, R. C., L. E. Monteith, C. A. Halgren, and P. C. Malte, "Molecular Nitrogen Yields from Fuel-Nitrogen in Backmixed Combustion," *Comb. Sci. and Tech.*, **19**, 95 (1979).

de Soete, G. G., "Overall Reaction Rates of NO and N_2 Formation From Fuel Nitrogen," Fifteenth Symposium (International) on Combustion, p. 1093, The Combustion Institute (1975).

Dunlap, R. W., and B. J. Goldsmith, "NSPS: Critique of Proposed Rulemaking," *Environmental Sci. and Tech.*, **13** (2), 172 (1979).

EPA, "Air Quality Criteria for Nitrogen Oxides," AP-84 (Jan., 1971).

Essenhigh, R. H., "Combustion and Flame Propagation in Coal Systems: A Review," Sixteenth Symposium (International) on Combustion, p. 353, The Combustion Institute (1977).

Fenimore, C. P., "Formation of Nitric Oxide from Fuel Nitrogen in Ethylene Flames," *Comb. Flame.*, **19**, 289 (1972).

Fenimore, C. P., "Reactions of Fuel-Nitrogen in Rich Flame Gases," *Comb. Flame*, **26**, 249 (1976).

Field, M. A., "Rate of Combustion of Size Graded Fractions of Char from a Low Rank Coal Between 1200°K," *Comb. Flame*, **13**, 237 (1969).

Field, M. A., "Measurements of the Effect of Rank on Combustion Rates of Pulverized Coal," *Comb. Flame*, **14**(2), 237 (1970).

Field, M. A., D. W. Fill, B. B. Morgan, and P. G. W. Hawksley, *Combustion of Pulverized Coal*, BCURA, Leatherhead, England (1967).

Gear, C. W., "The Automatic Integration of Ordinary Differential Equations," *Com. ACM*, **14**(3), 176 (1971).

Glassman, I., *Combustion*, Academic Press, New York (1977).

Haynes, G. S., "The Oxidation of Hydrogen Cyanide in Fuel-Rich Flames," *Comb. Flame*, **28**, 113 (1977).

Haynes, B. S., "Reactions of Ammonia and Nitric Oxide in the Burnt Gases of Fuel-Rich Hydrocarbon-Air Flames," *Comb. Flame*, **28**, 81 (1977).

Heap, M. P., et al., "Environmental Aspects of Low Btu Gas Combustion," Sixteenth Symposium (International) on Combustion, p. 535, The Combustion Institute (1977).

Horio, M., S. Mori, and I. Muchi, "A Model Study for the Development of Low NO_x Fluidized Bed Coal Combustors," Proceedings of the Fifth International Conference on Fluidized Bed Combustion, **II**, Washington, DC (December, 1977).

Howard, J. B., G. C. Williams, and D. H. Fine, "Kinetics of Carbon Monoxide Oxidation in Postflame Gases," Fourteenth Symposium (International) on Combustion, p. 975, The Combustion Institute (1973).

JANAF Thermochemical Tables, Dow Chemical Co., Midland, Michigan (1965).

Jensen, D. E., and G. A. Jones, "Reaction Rate Coefficients for Flame Calculations," *Comb. Flame*, **32**,1 (1978).

Kobayashi, H., J. B. Howard, and A. F. Sarofim, "Coal Devolatilization at High Temperatures," Sixteenth Symposium (International) on Combustion, p. 411, The Combustion Institute (1977).

Lachapelle, D. G., J. S. Bowen, and R. D. Stern, "Overview of Environmental Protection Agency's Nitrogen Oxide Control Technology for Stationary Combustion Sources," *AIChE Symp. Ser.*, No. 156, **72**, 263 (1976).

Lavoie, G. A., J. B. Heywood, and J. C. Keck, "Experimental and Theoretical Study of Nitric Oxide Formation in Internal Combustion Engines," *Comb. Sci. and Tech.*, **1**, 313 (1970).

Lowe, A., T. F. Wall, and I. M. Stewart, "Combustion Kinetics in the Modeling of Large, Pulverized Fuel Furnaces: A Numerical Experiment in Sensitivity," *AIChE J.*, **23**(4), 440 (1977).

Marquardt, D. W., "An Algorithm for Least Squares Estimation of Nonlinear Parameters," *J. Soc. Indust. Appl. Math.*, **11**, 431 (1963).

Martin, G. B., and E. E. Berkau, "An Investigation of the Conversion of Various Fuel Nitrogen Compounds to Nitrogen Oxides in Oil Combustion," paper presented at *Symposium on Combustion Processes and Air Pollution Control*, AIChE 70th Annual Meeting, Atlantic City (1971).

Menster, M., H. S. O'Donnell, S. Ergun, and R. A. Friedel, "Devolatilization of Coal by Rapid Heating," *Adv. Chem. Ser.*, No. 131 (1973).

Mitchell, J. W., "A Kinetic Model of Nitric Oxide Formation in Pulverized Coal Combustion," M.S. Thesis, The Pennsylvania State University (1980).

Morley, C., "The Formation and Destruction of Hydrogen Cyanide From Atmospheric and Fuel Nitrogen in Rich Atmospheric-Pressure Flames," *Comb. Flame*, **27**, 189 (1976).

Muzio, L. J., J. K. Arand, and D. P. Teixeira, "Gas Phase Decomposition of Nitric Oxide in Combustion Products," Sixteenth Symposium (International) on Combustion, p. 199, The Combustion Institute (1977).

Newhall, H. K., and S. M. Shahed, "Kinetics of Nitric Oxide Formation in High-Pressure Flames," Thirteenth Symposium (International) on Combustion, p. 381, The Combustion Institute (1971).

PAT Report, "A Way to Lower NO_x in Utility Boiler," *Environmental Sci. and Tech.*, **11**(3), 226 (1977).

Pershing, D. W., and J. O. L. Wendt, "Pulverized Coal Combustion: The Influence of Flame Temperature and Coal Composition on Thermal and Fuel NO_x," Sixteenth Symposium (International) on Combustion, p. 389, The Combustion Institute (1977).

Pohl, J. H. and A. F. Sarofim, "Devolatilization and Oxidation of Coal Nitrogen," Sixteenth Symposium (International) on Combustion, p. 491, The Combustion Institute (1977).

Pompei, F., and J. B. Heywood, "The Role of Mixing in Burner Generated Carbon Monoxide and Nitric Oxide," *Comb. Flame*, **19**, 407 (1972).

Rajan, R., and C. Y. Wen, "A Comprehensive Model for Fluidized Bed Coal Combustors," *AIChE J.*, **26**(4), 642 (1980).

Sarofim, A. F., J. H. Pohl, and B. R. Taylor, "Strategies for Controlling Nitrogen Oxide Emissions During Combustion of Nitrogen-Bearing Fuels," *AIChE Symp. Ser.*, No. 148, **74**, 67 (1978).

Sarofim, A. F., and R. C. Flagan, "NO_x Control for Stationary Combustion Sources," *Prog. Energy Comb. Sci.*, **2**, 1 (1976).

Sarofim, A. F., G. C. Williams, M. Modell, and S. M. Slater, "Conversion of Fuel Nitrogen to Nitric Oxide in Premixed and Diffusion Flames," *AIChE Symp. Ser.*, No. 148, **71**, 51 (1976).

Sawyer, R. F., and I. Glassman, "The Reactions of Hydrogen with Nitrogen

Dioxide, Oxygen, and Mixtures of Oxygen and Nitric Oxide," Twelfth Symposium (International) on Combustion, p. 469, The Combustion Institute (1969).

Solomon, P. R., and M. B. Colket, "The Evolution of Fuel Nitrogen in Coal Devolatilization," Unpublished Report (1978).

Sternling, C. V. and J. O. L. Wendt, "Kinetic Mechanisms Governing the Fate of Chemically Bound Sulfur and Nitrogen in Combustion," EPA-650/2-74-017 (1972).

Tarbell, J. M., and C. A. Petty, "Combustion Modifications for the Control of NO_x Emissions," *Chem. Engr. Sci.*, **32**(10), 1177 (1977).

Vogt, R. A., and N. M. Laurendeau, "Nitric Oxide Formation in Pulverized Coal Flames," Report No. PURDU-CL-76-8, Prepared for the National Science Foundation under Grant GK-42141 (1976).

Weekman, V. W., "Lumps, Models, and Kinetics in Practice," *AIChE Monograph Series*, **75** (1979).

Wen, C. Y., and St. Tone, "Coal Conversion Reaction Engineering," *ACS Symp. Ser.*, **72**, p. 56 (1978).

Wen, C. Y., R. C. Bailie, C. Y. Lin, and W. S. O'Brien, "Production of Low Btu Gas Involving Coal Pyrolysis and Gasification," *Adv. Chem. Ser.*, No. 131, p. 9 (1973).

Wendt, J. O. L., and D. W. Pershing, "Physical Mechanisms Governing the Oxidation of Volatile Fuel Nitrogen in Pulverized Coal Flames," *Comb. Sci. and Tech.*, **16**, 111 (1977).

Wendt, J. O. L., and O. E. Schulze, "On the Fate of Fuel Nitrogen During Coal Char Combustion," *AIChE J.*, **22**(1), 102 (1976).

Westenberg, A. A., Kinetics of NO and CO in Lean, Premixed Hydrocarbon-Air Flames," *Comb. Sci. and Tech.*, **4**, 59 (1971).

Williams, G. C., H. C. Hottel, and A. C. Morgan, "The Combustion of Methane in a Jet-Stirred Reactor," 12th Symposium (International) on Combustion, p. 913, The Combustion Institute (1976).

Zeldovich, J., "The Oxidation of Nitrogen in Combustions and Explosions," *Acta Physicochimica URSS*, **21**, 577 (1946).

Zimont, V. L., and Yu. M. Trushin, "Total Combustion Kinetics of Hydrocarbon Fuels," *Comb. Explosion and Shock Waves*, 5(4), 391 (1969).

Manuscript received May 16, 1980; revision received April 30, and accepted May 15, 1981

Three-Dimensional, Randomized, Network Model for Two-Phase Flow through Porous Media

A structural model for a porous medium in the form of a randomized, three-dimensional network is developed that can be used to calculate permeability, capillary pressure as measured under static conditions and during steady-state flows, and relative permeabilities as measured during steady-state flows.

This randomized network model, expressed in terms of seven free parameters, can be employed to correlate for a given system the single-phase permeability, the drainage and imbibition capillary pressure curves, and the two drainage relative permeability curves. The subsequent portions of the hysteresis loops for capillary pressure and for the relative permeabilities then can be predicted.

The limited data available from the literature for unconsolidated packed beds have been successfully correlated: 100 to 200 mesh sand and uniform 181 μm glass spheres. Data for a bed of sintered 200 μm glass beads also has been successfully described.

CHENG-YUAN LIN
and
JOHN C. SLATTERY
Department of Chemical Engineering
Northwestern University
Evanston, IL 60201

SCOPE

The configuration of the pore space in a permeable rock, in a bed of sand, or in an irregular bed of spheres will normally be at least in part a random function of position in space. Although the usual equations of motion are believed applicable to each phase moving through an individual pore, they can not be solved, because an a priori description of the necessary boundary conditions is not possible.

The usual approach in avoiding this difficulty is to speak in terms of averaged variables. Formally, local volume averages of the equations of motion for each phase can be written that are valid for each point within a multiphase flow through a permeable structure. The advantages are that all local volume averaged variables are continuous functions of position in space and that detailed configurations for all of the various phase interfaces are no longer required.

The disadvantage is that in place of this lost information we have several integrals, descriptions for which must be given before we can proceed further. For a two-phase flow through a porous medium in the absence of interphase mass transfer, these integrals are the permeability to a single phase, the relative permeability for each phase, and the capillary pressure.

In describing these integrals, one can rely strictly on empiricism or correlations of experimental data. This is not entirely satisfactory, since there are many interacting physical phenomena.

Here we have adopted another approach in which these integrals are modelled through the introduction of an idealized structural model for the pore space bounded by the local averaging surface defined at each point within the porous medium. The model we have adopted is a three-dimensional, randomized network of sinusoidal pores. At each node in the network, we require mass conservation and continuity of pressure for each phase. A Beta probability density function is used to describe the distribution of the pore neck radii.

Such a model has not been used previously. Fatt (1956,a,b,c) employed a regular, two-dimensional network of cylindrical pores. His model was modified by Dodd and Kiel (1959) to allow

---

0001-1541-82-5240-0311-$2.00.